A Novel Multilayer EBG Structure to Reconfigure the Band-Notch of UWB Monopole Printed Antenna

Kompella S. L. Parvathi* **and Sudha R. Gupta**

Abstract—In high speed indoor communication, ultra-wideband (UWB) plays a crucial role. UWB contains several other narrow band systems, which give interference. In order to reject these narrow bands present in UWB system, a novel multilayer step via electromagnetic band gap (MS-EBG) structure to vary the band-notch of UWB monopole printed antenna is presented in this work. The proposed EBG consists of grooved substrate with step via arrangement. These grooved substrate allow for the deposition of the liquids with different dielectric constants to achieve the variations in band gap center frequency of EBG. The microstrip line based model with equivalent circuit diagram of MS-EBG is developed with experimental results using suspended microstrip line (SML) method, with different liquids like kerosene, sea water, mineral oil, without grooved substrate, etc. The simulated and experimental results show liquid sensing ability of the proposed MS-EBG structure. The application of MS-EBG to vary the band notch in UWB hexagonal monopole antenna (HMA) is also demonstrated. Simulated and experimental results show noticeable variation in the band notch center frequency with different liquids deposited in the grooved substrate. The proposed method required only liquid change arrangement to get desired band notch in UWB monopole antenna. Compared to electrical and mechanical method to get band notch in UWB monopole antenna, the proposed method works without any power supply, active devices, and additional complex arrangement.

1. INTRODUCTION

Ultra-wideband (UWB) system plays an important role in high speed indoor communication due to its support to high data rate, low transmitted power requirement, etc. [1, 2]. UWB contains several other narrow band systems like wireless local area network (WLAN) (5.150–5.350 GHz; 5.725–5.825 GHz), WiMAX (2.500–5.690 GHz; 3.400–3.690 GHz; 5.250–5.825 GHz), etc., which gives interference. In order to reject these unwanted interferences, UWB antennas with notch band are required to design. As per reported work, printed monopole antenna is the key antenna for a UWB system [1, 2].

Several methods are proposed to reject these unwanted narrow bands. The conventional methods are cutting slots on the radiating element/ground plane [3–5], placing parasitic elements near radiating element [6–8], use of fractal tuning stub [9], using quarter wavelength tuning stub [10], utilizing small resonant radiating element [11], placing resonant cell in the microstrip feedline [12], etc. Placing an electromagnetic band gap structure (EBG) near the feed line of an antenna exhibits advantages like less effect on radiation performance on un-notch frequencies, less coupling effect, etc. [13–16]. However, fixed band rejection is not constantly required, rather variable band rejection is required.

As per demand of variable band notch UWB antennas, recently several UWB monopole antennas with variable band rejection using electrical method [17–21], radio frequency micro electro mechanical systems (RF-MEMS) [22, 23], optically controlled switches [24, 25], mechanical methods [26] are

proposed. Electrical method to get band notch in UWB printed monopole antenna requires direct current (dc) to bias the switch component and battery with the antenna module. Optical controlled method requires arrangement to build and control optical switches which occupies extra space. Mechanically band notch variable UWB antenna requires additional network to control, which increases cost, weight, complexity, limiting the performance of antenna in portable applications. To overcome the limitations of these reported methods to get variable band notch in UWB monopole printed antenna, in this work an EBG as a sensor for different liquids [27] is adopted to get variable band notch UWB antenna by placing single unit cell of multilayer step via EBG (MS-EBG) near the feed line. The proposed method to get variable band notch in UWB monopole antenna works without any additional dc power supply, controlling switches, and mechanical arrangement.

The paper is organised as follows. The geometry of unit cell of the proposed multilayer step via EBG (MS-EBG) structure, dispersion diagram, and experimental results using SML methods are presented in Section 2. Application of the proposed MS-EBG structure to get the variation in band notch for UWB monopole antenna is demonstrated in Section 3. The paper is concluded in Section 4 with comparison of different reported methods to get band notch in UWB printed monopole antenna.

2. PROPOSED MULTI LAYER STEP VIA EBG (MS-EBG) STRUCTURE

The unit cell design with its equivalent circuit model, dispersion diagram analysis, and band gap measurement using microstrip line are discussed in the following subsections.

2.1. Unit Cell Design and Equivalent-Circuit Model

The multilayer EBG structure can be represented as an equivalent parallel LC resonance circuit [28–30]. The resonance frequency (f_c) of parallel LC circuit is given as

$$f_c = \frac{1}{2\pi\sqrt{LC}} \tag{1}$$

Inductance (L) and capacitance (C) are given as

$$L = 0.2h\left[\ln\left(\frac{2h}{r}\right) - 0.75\right] \tag{2}$$

and

$$C = \epsilon_o\epsilon_r\frac{a^2}{h} \tag{3}$$

where (μ_0) = permeability of free space, (h) = total substrate height, (a) = width of each EBG patch, (g) = gap between two adjacent EBG cells, (ϵ_r) = dielectric constant of the substrate, and (ϵ_0) = permittivity of free space. The bandgap bandwidth (BW) of EBG structure is given as

$$BW = \frac{1}{\eta}\sqrt{\frac{L}{C}} = \frac{\Delta\omega}{\omega_o} \tag{4}$$

$$Z_s = \frac{j\omega L}{1 - \omega^2 LC} \tag{5}$$

where η is the free space impedance. The (C) is due to the gap between two EBG patches and (L) due to current path from via-ground-plane-via of the adjacent cell. From Eq. (1), in order to achieve tunable EBG structure, the product of LC should be varied. In this work, this variation is achieved by using different liquids with different dielectric constants. The geometry of the unit cell of proposed MS-EBG is shown in Figure 1. The unit cell consists of a three layer substrate with uniform height, and the top layer of the substrate consists of a square ring patch and an inner square patch of conducting material. The substrate between square ring and square patch of the top layer is grooved with depth of $b_2 = 0.8$ mm to deposit different liquids. Layer-1 consists of an offset via with radius (r) = 0.2 mm with perfect electric conductor (PEC) block with dimensions $a_1 = 3.2$ mm, $b_1 = 0.5$ mm, $S_5 = 0.4$ mm, respectively, placed on layer-1 as shown in Figure 1. Layer-2 consists of a center located via with another
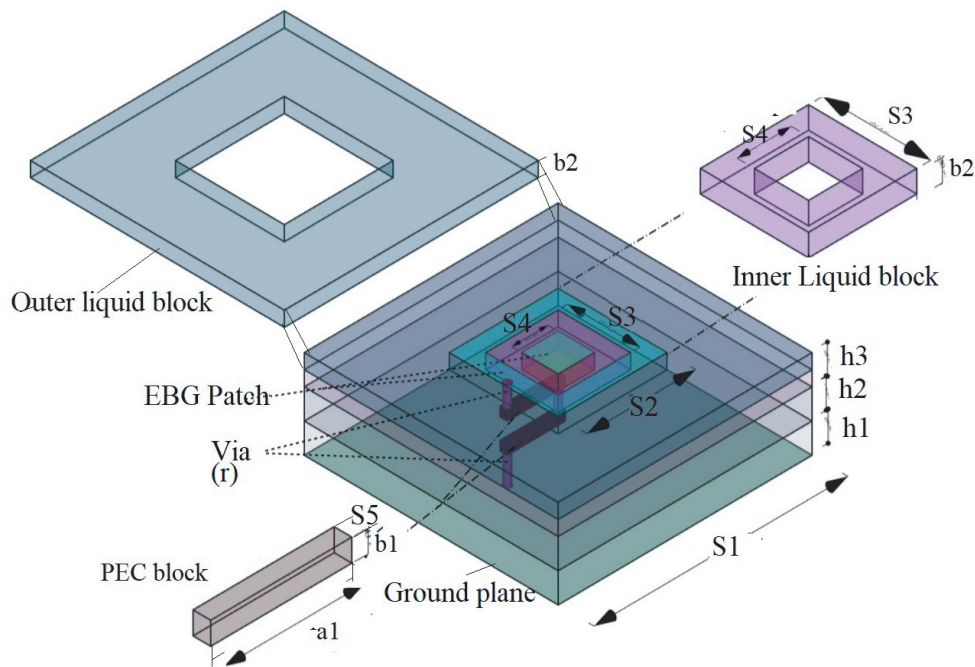
Figure 1. 3-D geometry of the proposed multilayer sensor electromagnetic band gap structure (MS-EBG) $(a_1, b_1, b_2, S_1, S_2, S_3, S_4, S_5, h_1, h_2, h_3, r) = (3.2\,\text{mm}, 0.5\,\text{mm}, 0.8\,\text{mm}, 14\,\text{mm}, 6\,\text{mm}, 4\,\text{mm}, 2\,\text{mm}, 0.4\,\text{mm}, 1.6\,\text{mm}, 1.6\,\text{mm}, 1.6\,\text{mm}, r = 0.2\,\text{mm}.)$.

PEC block with same dimensions on layer-2, to establish the path between ground and outer ring patch. Layer-3 consists of another offset via similar to layer-1. PEC block gives current path by connecting the via of each layer. This step via arrangement is done to get a compact EBG cell [31].

Microstrip line based model is used to define the characteristics of proposed EBG [13]. As shown in Figure 2, capacitance C_1 is due to the coupling between the outer ring and microstrip line, by changing
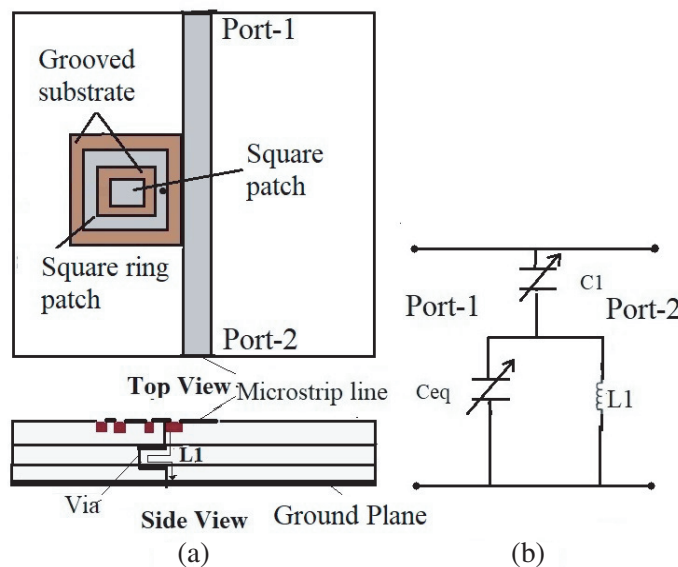

Figure 2. Microstrip-line-based model. (a) Configuration schematic view, and (b) Equivalent-circuit model.

the liquid in the grooved substrate between microstrip line, and outer ring of the EBG patch C_1 is varied without changing the physical dimensions. Inductance L_1 is due to the via in each layer and two PEC blocks. C_{eq} is varied due to the different liquid characteristics present in the grooved substrate [32] around the inner patch and square ring patch. The resonance frequency f_c of the proposed MS-EBG is given as [28, 30].

$$f_c = \frac{1}{2\pi\sqrt{L(C_{eq} + C_1)}} \tag{6}$$

where C_{eq} and C_1 depend on liquid properties and the depth of the grooved substrate.

2.2. Simulation Results and Parametric Analysis

To study the variation in f_c due to C_{eq} and C_1 with different liquids, unit cell of the proposed MS-EBG is simulated in the eigen mode solution of ANSYS high frequency structure simulator (HFSS) [34]. The different parameters of the unit cell of MS-EBG are mentioned in Figure 1. One-dimensional dispersion diagrams for no sample, kerosene, sea water in the grooved substrate of the MS-EBG and for without grooved substrate are shown in Figure 3. As shown in Figure 3(a) when there is no sample in grooved substrate band gap is observed with center frequency $f_c = 3.27\,\text{GHz}$. When the grooved substrate is filled with kerosene, sea water, f_c is observed at $3.21\,\text{GHz}$ and $1.95\,\text{GHz}$, respectively. As shown in Figure 3(b), when there is no groove in substrate band gap center frequency is observed at $3.09\,\text{GHz}$. Simulated result shows the liquid sensing capability of the proposed MS-EBG.

To analyze the effect of depth of grooved substrate (b_2) and number of substrate layers (N) on band gap centre frequency (f_c) and band gap band width (BW), 1×8 cells of MS-EBG have been simulated using ANSYS HFSS [35] with no sample (air, $\epsilon_r = 1$) in a grooved substrate. The 1×8 cells are developed on a 3 layer substrate with $\epsilon_r = 4.4$, $\tan\delta = 0.02$ and $h_1 = h_2 = h_3 = 1.6\,\text{mm}$ using suspended microstrip line (SML) method [36] with other parameters of the MS-EBG kept the same as mentioned earlier. Simulated (f_c) for different grooved substrate depths (b_2) and numbers of layers (N) are given in Table 1. It is observed that as the depth of the groove increases the bandgap bandwidth also increases. As shown in Table 1, if the number of layer increases, reduction in f_c is observed.

Table 1. Effect of grooved substrate depth $(b_2\,\text{mm})$ and number of layers (N) of MS-EBG on band gap bandwidth (BW, %) and band gap center frequency $(f_c\,\text{GHz})$ (no sample, $\epsilon_r = 1$.).

Effect of b_2					Effect of N				
b_2	f_l	f_h	BW	f_c	N	f_l	f_h	BW	f_c
0.4	2.22	3.27	38.32	2.74	2	2.11	3.32	44.64	2.71
0.8	2.12	3.45	47.67	2.79	3	2.12	3.45	47.67	2.79
1.2	2.06	3.49	51.62	2.77	4	1.64	2.89	51.30	2.26
1.4	2.12	3.69	54.13	2.90	5	1.47	2.72	59.80	2.09

2.3. Experimental Results and Validation

To verify the liquid sensing ability of proposed MS-EBG structure, it is fabricated by using standard printed circuit board (PCB) technology. 1×8 MS-EBG has been printed on an FR4 substrate with $\epsilon_r = 4.4$, $\tan(\delta) = 0.02$, and height of each layer $1.6\,\text{mm}$ using SML method with other parameters as mentioned in Figure 1. The measurement of S_{12} is carried out in following way [32]

- To avoid the leakage of liquids deposited in the grooved substrate adhesive masking tapes are used [32].
- Liquids are injected using injection to avoid the leakage of liquids [33].
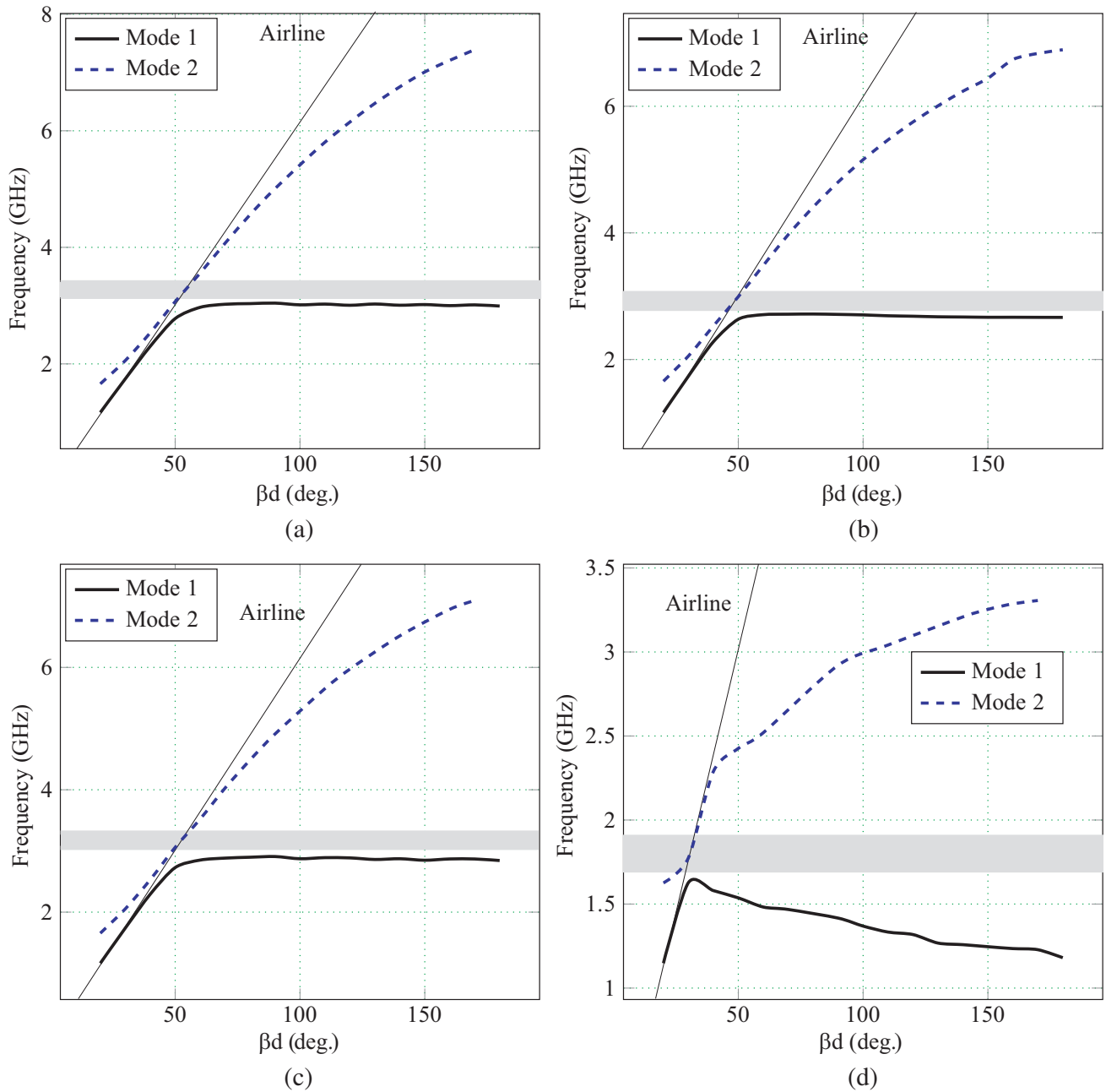- Measurements are carried out at 25^0 temperature and in the middle of the room.

Figure 3. Dispersion diagram of proposed MS-EBG for different liquids placed in grooved substrate. (a) No sample (air, $\epsilon_r = 1$), (b) no grooved on substrate (FR4, $\epsilon_r = 4.4$), (c) Kerosene ($\epsilon_r = 2.09$), and (d) sea water ($\epsilon_r = 80$).

- To observe the effect adhesive masking tapes on the performance of proposed EBG, measurements are carried out with and without adhesive masking tapes, and negligible effects are observed.

Measurement setup of the proposed MS-EBG is shown in Figure 4. To achieve feasibility in the change of liquid in practical use, the method adopted in [32, 33] is considered in the experiment work. Measured S_{12} for no sample, kerosene, seawater, mineral oil, etc. which are presented in Figure 5, and the fabrication without grooved substrate is also carried out. From the measured S_{12} with no sample in the grooved substrate, the bandgap BW with $f_l = 2.15\,\text{GHz}$, $f_h = 3.42\,\text{GHz}$ for ($S_{12} < -20\,\text{dB}$) [36] is observed while for kerosene, sea water, mineral oil and without grooved substrate bandgap center

frequencies (f_c) are observed at 2.75 GHz, 1.78 GHz, 2.73 GHz, and 2.61 GHz, respectively. As shown in Figure 5, band gap center frequency of MS-EBG for sea-water is shifted by approximately 1 GHz due to its high dielectric constant value compared to other liquids which are used in the experiment. Simulated and measured results agreed well as shown in Figure 5. There are minor deviations which are negligible and observed due to fabrication errors, boundary between liquids, infinite boundary conditions in simulation and FR4 substrate, multilayer substrate, etc. Simulated and measured results show the liquid sensing capability of the proposed MS-EBG structure using different liquids with different dielectric properties which is very useful in reconfigurable antennas and microwave engineering [32].
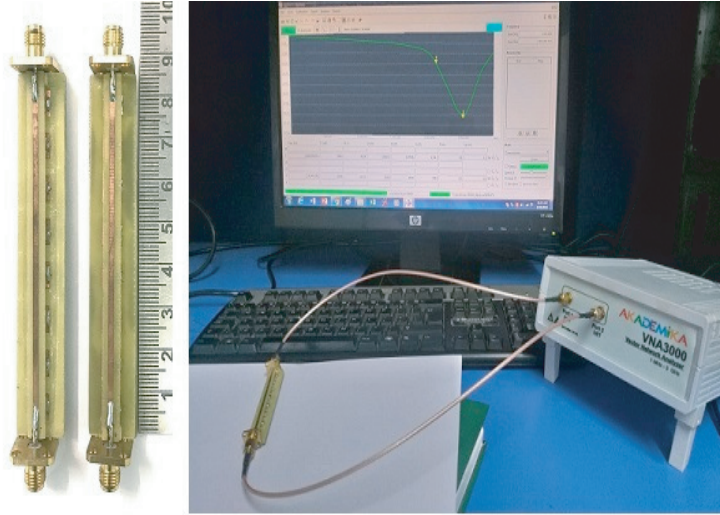

Figure 4. Measurement setup using suspended micro strip line method for proposed MS-EBG for no sample ($\epsilon_r = 1$).
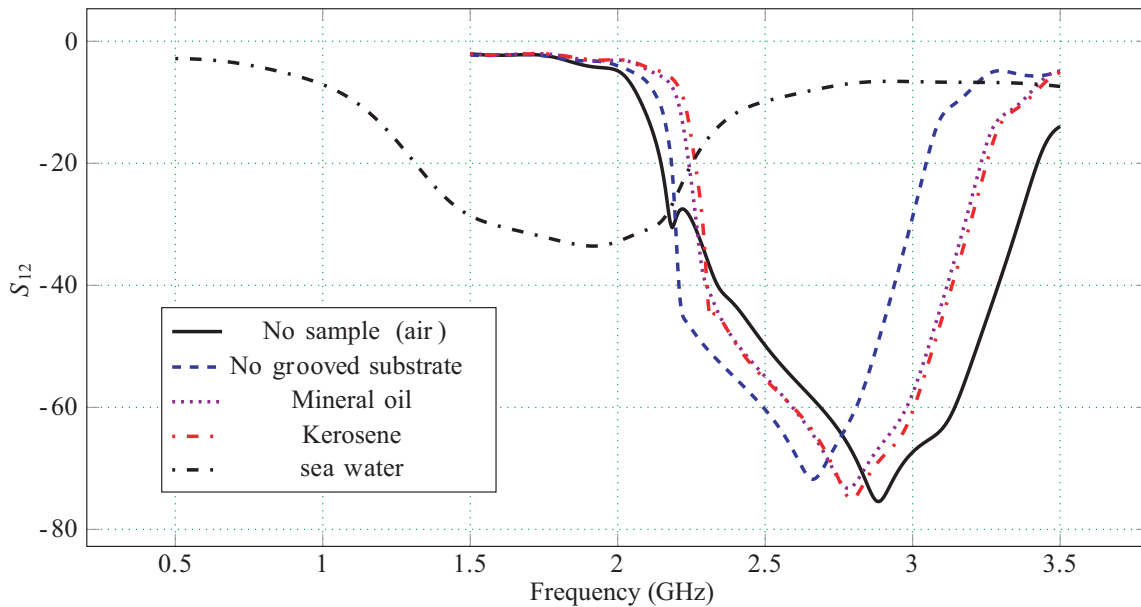

Figure 5. Measured S_{12} using suspended micro strip line method for proposed MS-EBG for different liquids deposited in grooved substrate.

3. APPLICATION

An application of the proposed MS-EBG structure to vary the band notch of the UWB monopole antenna and its practical demonstration are discussed in the following subsections.

3.1. UWB Two Layer Hexagon Monopole Antenna

A standard printed two layer hexagon monopole antenna (HMA) [37] with a microstrip feed line is used as a base antenna. A two layer hexagon monopole antenna is shown in Figure 6(a) with parameters used for further design as substrate $\epsilon_r = 4.4$, $\tan(\delta) = 0.02$. The antenna is composed of a hexagonal shape radiator and microstrip feed line printed on a two layer substrate with uniform height of each layer $(h_1) = (h_2) = 0.8$ mm. The dimensions of the HMA and ground planes are mentioned in Figure 6.
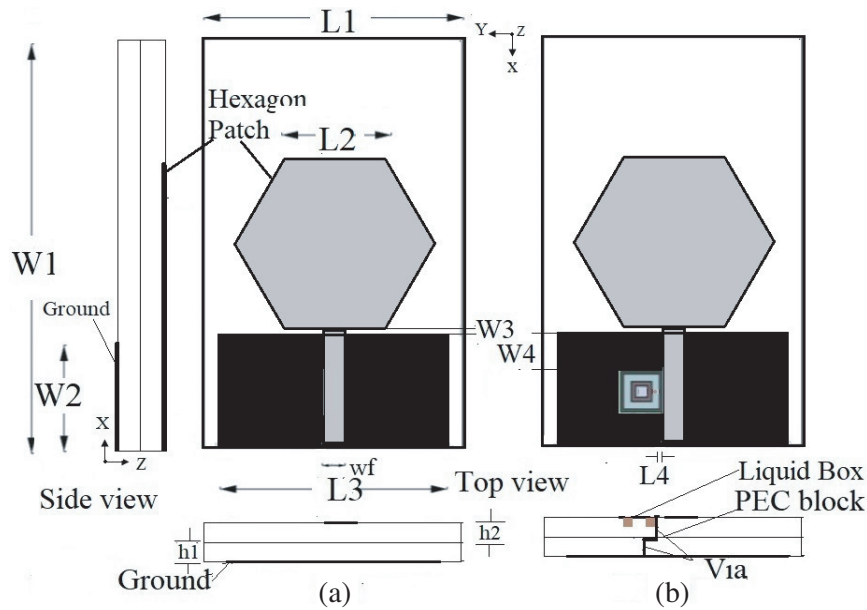

Figure 6. Configuration of UWB hexgonal monopole antenna, (a) without MS-EBG, and (b) with MS-EBG (L_1, L_2, L_3, L_4, W_1, W_2, W_3, W_4, S_1, S_2, S_3, S_4, S_5, a_1, b_1, b_2, h_1, h_2, $= 32$ mm, 12.48 mm, 28 mm, 0.3 mm, 52 mm, 13.5 mm, 0.5 mm, 3.72 mm, 5.1 mm, 4.5 mm, 2.5 mm, 1.5 mm, 0.4 mm, 2.05 mm, 0.2 mm, 0.4 mm, 0.8 mm, 5.1 mm.).

The simulated VSWR of the two layer HMA is shown in Figure 7. In the UWB (3.1–10.6 GHz), good impedance is observed with $VSWR < 2$ without any band notch.

3.2. Single Notch UWB HMA with MS-EBG

The baseline structure of the two layer HMA with unit cell of MS-EBG is shown in Figure 6(b) with different liquids in the grooved substrate simulated using HFSS. The parameters of the HMA with single cell of MS-EBG are shown in Figure 6. The substrate parameters are $\epsilon_r = 4.4$, $\tan(\delta) = 0.02$, $h_1 = 0.8$ mm, $h_2 = 0.8$ mm. Simulated VSWRs of the HMA with MS-EBG for different liquids in the grooved substrate are shown in Figure 7. Simulated results show good impedance matching $VSWR < 2$ throughout the UWB except for the narrow notch band due to the resonance of the MS-EBG. The simulation results also show that the frequency of the notch band can be varied by changing the liquids in the grooved substrate of the MS-EBG where several narrow band interferes exist. From the simulation results it is also observed that placing the MS-EBG near the feed line and changing of liquids in the grooved substrate of the MS-EBG have negligible effect on the response of the antenna other than notch band frequency. The effect of different ϵ_r on band notch of HMA with MS-EBG is shown in
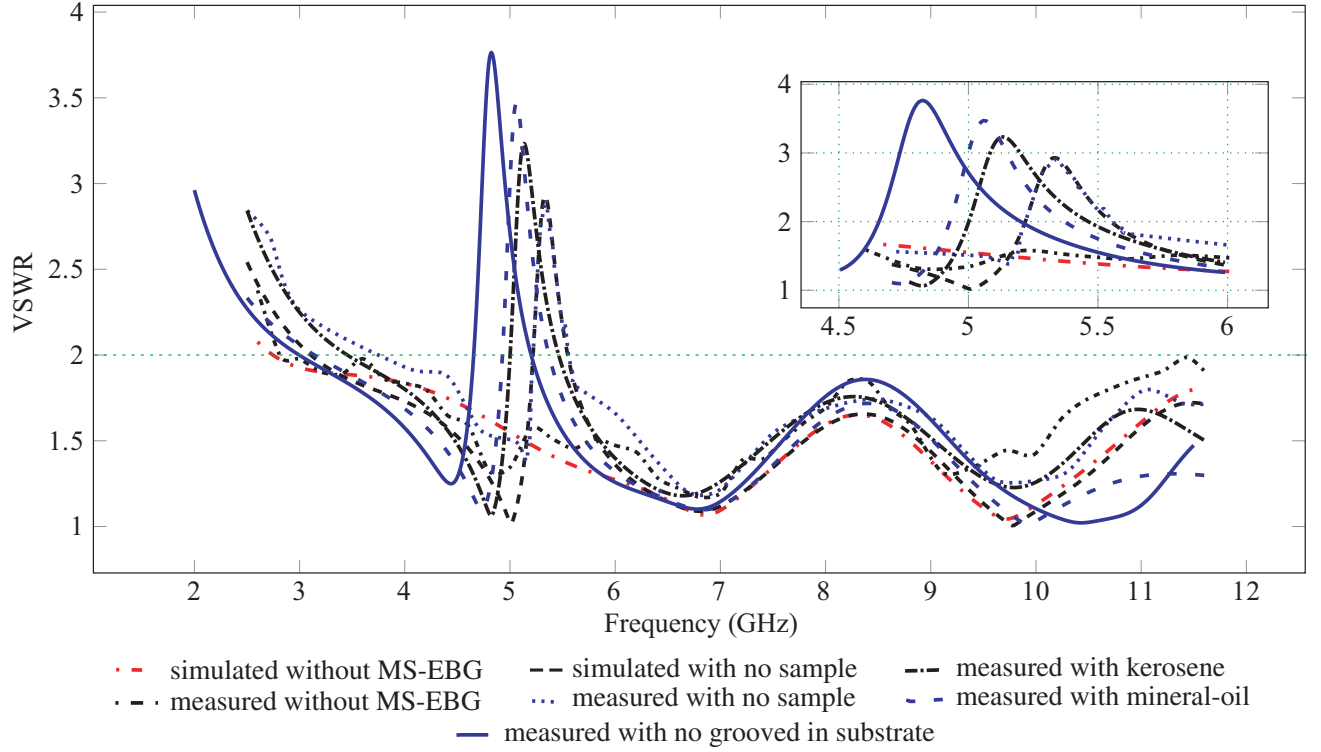
Figure 7. Simulated, and measured VSWR of UWB HMA without and with MS-EBG for different liquids placed in grooved substrate.
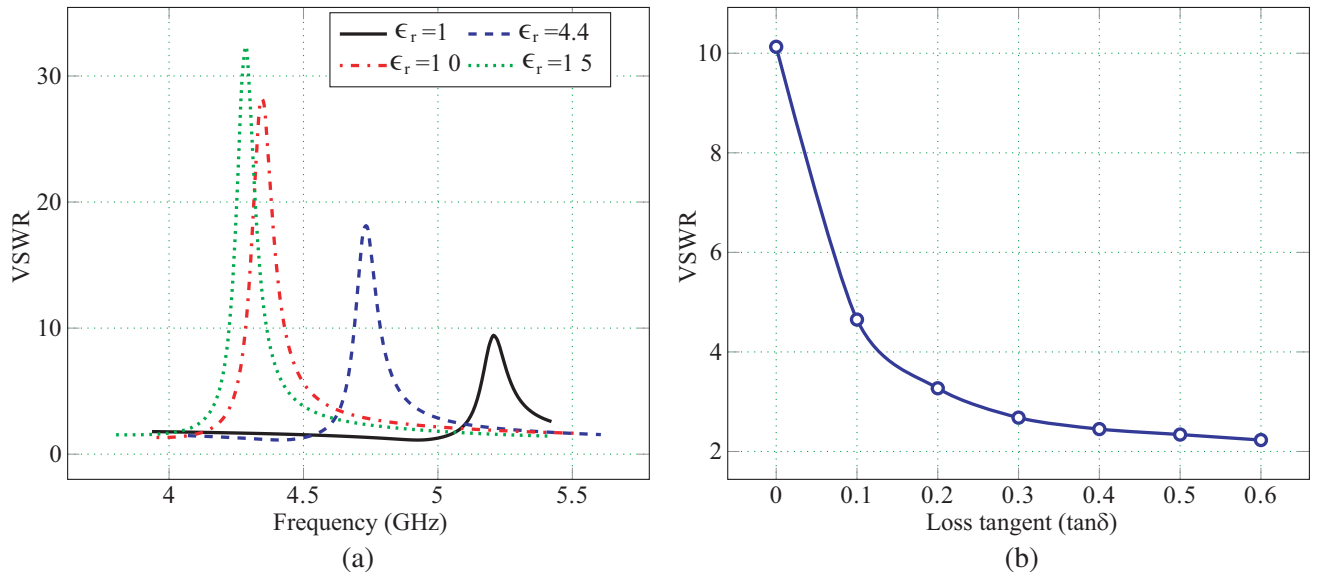

Figure 8. (a) Effect of Different ϵ_r present in the grooved substrate on band notch of the HMA with MS-EBG. (b) Dependence of the band-notch VSWR value on loss $\tan \delta$.

Figure 8(a). From Figure 8(a) it is observed that with the increase in ϵ_r, band notch shifts towards the lower frequency. In Figure 8(b), dependency of the band-notch VSWR value on $\tan \delta$ is demonstrated. It is noticed that with the increase in the loss tangent value notch band VSWR value decreases. From Figures 8(a) and (b) it is clear that HMA with MS-EBG follows the state of art to get notch band in

Table 2. Effect of loss tangent on band notch center frequency, VSWR, and bandwidth of band notch with $\epsilon_r = 1$.

Loss tangent $(\tan \delta)$	Notch-band Center freq. (GHz)	VSWR	Notch-band Bandwidth
0	5.28	10.13	5.13 GHz–5.59 GHz
0.1	5.27	4.65	5.14 GHz–5.55 GHz
0.2	5.30	3.27	5.17 GHz–5.54 GHz
0.3	5.31	2.68	5.19 GHz–5.52 GHz
0.4	5.34	2.45	5.22 GHz–5.48 GHz
0.5	5.34	2.34	5.25 GHz–5.44 GHz
0.6	5. 32	2.23	5.26 GHz–5.43 GHz
0.7	5. 31	2.14	5.29 GHz–5.39 GHz
0.8	5. 30	2.06	5.32 GHz–5.37 GHz
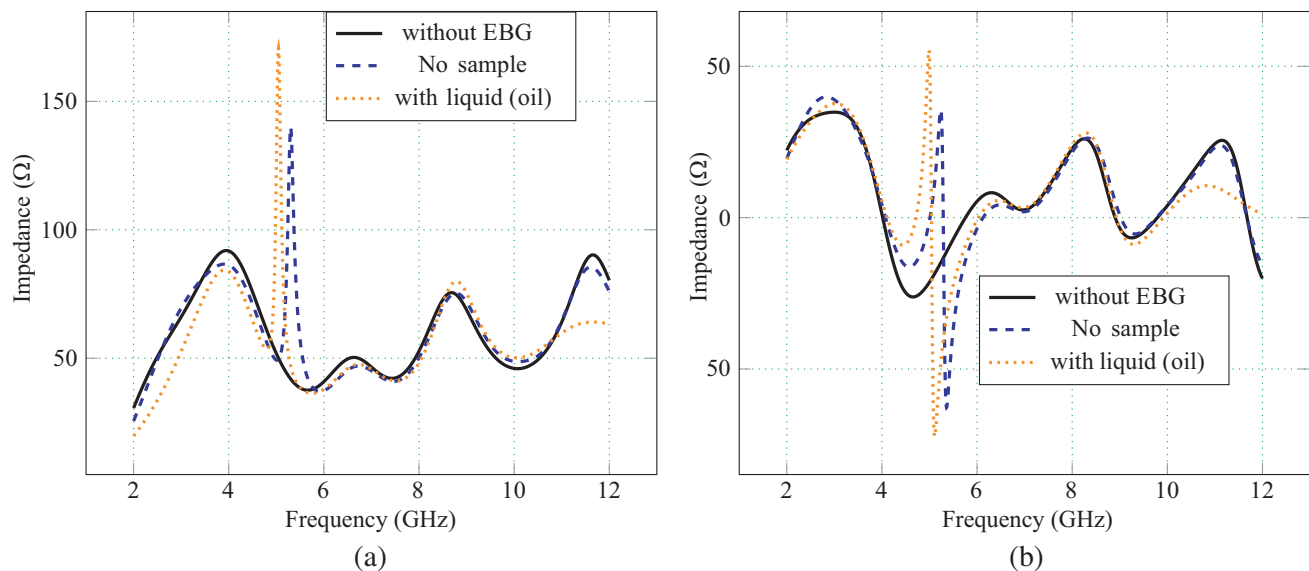
Figure 9. Impedance of HMA with and without MS-EBG. (a) Real, and (b) Imaginary.

UWB monopole printed antenna. The detailed study of effect of different loss tangent values on band gap center frequency and bandwidth of band notch is provided in Table 2. From Table 2, it is clear that the increase in the loss tangent value decreases the VSWR value at notch band, and very small shifting (5.27–5.32 GHz) is observed. Simulated impedance of the HMA with MS-EBG (with mineral oil and no sample) is demonstrated in Figure 9. Loading of MS-EBG near feedline real part of impedance is away from 50 Ω and imaginary part away from 0 Ω for band notch frequency. The maximum gain of the HMA with MS-EBG (no sample and mineral oil in grooved substrate) is shown in Figure 10(a) which shows reduction in the gain at the band notch frequency for different liquids and good performance for other frequencies.

   To study the effect of the proposed technique in the time domain characteristics, a pair of HMAs with EBG and without EBG (face to face) with no sample, mineral oil, and kerosene in the grooved substrate with distance 100 mm from each other are simulated, and the transmission group delay is plotted in Figure 10(b). A small variation of the group delay in un-notched frequency band shows the linear phase in the far field region and no sensible pulse distortion at the UWB. Small variations

Table 3. Comparasion of proposed method with other method to get band notch in UWB printed monopole antenna.

Ref.	Notch band mechanism	ϵ_r/h (mm)	No. of notch	Additional devices to get reconfiguration	Variation in Notch (GHz)	Min. VSWR value in Band Notch
[17]	Electrical	2.2/0.787	02	Varactor diode, U-shaped Parasitic element	6.175–6.35	6.3
[18]	Electrical	2.2/0.257	01	Varactor diode S-SSR at feed line.	3.1–5.6	8
[19]	Electrical	4.4/0.8	02	PIN diode, Inverted U-Shaped slots.	Switchable	5.2
[21]	Electrical and EH	2.2/0.787	01	FET, EH system.	Switchable	5.0
[22]	RF-MEMS	3/0.1	01	RF-MEMS switch, U-Shaped slot, L-Shaped stubs.	Switchable	NM
[23]	RF-MEMS	3.9/N.M.	01	RF-MEMS switch, $\lambda/4$ open circuit feed stubs.	Switchable	NM
[24]	Optical controlled	4.4/0.8	01	Photo conductive switch, folded slot U-shaped slot.	Switchable	4.4
[25]	Optical controlled	4.6/1.5	02	OCMS, CSRR on the radiating element.	Switchable	6
[26]	Mechanical	2.33/1.575, 2.33/1.575	01	PIN diodes, SRR at feed line, servo motor, aurdino unit microcontroller	Switchable	NM
P.W.	**Liquid change**	**4.4/0.8 4.4/0.8**	**01**	**Different liquids with different ϵ_r, unit cell of MS-EBG at feed line**	**4.78–5.38**	**3**

P. W. = Propose work, OCMS = Optical controlled microwave switch, S-SSR = S-Shaped Split-Ring Resonators, EH = Energy harvesting, CSRR = Complementary split-ring resonators, SRR = split-ring resonator, RF-MEMS = Radio frequency micro electro mechanical systems, NM = Not mentioned.
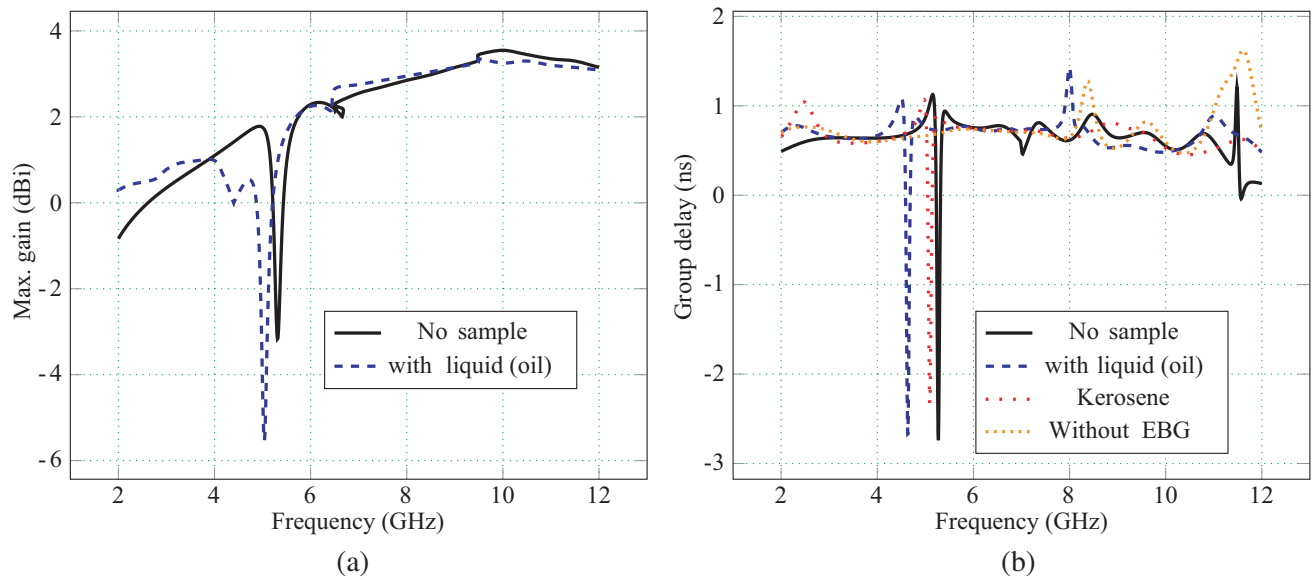
Figure 10. (a) Maximum realized gain, and (b) Group delay of HMA with MS-EBG.
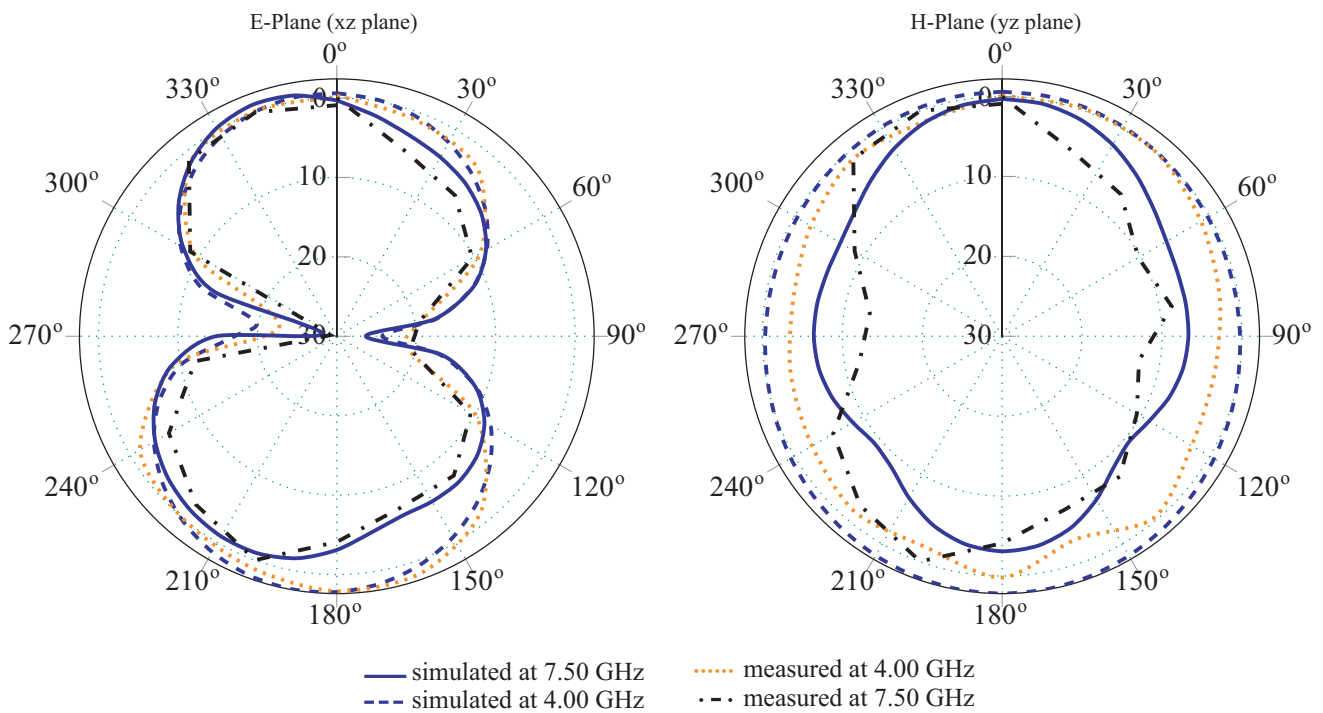

Figure 11. Simulated and measured radiation pattern of the HMA with MS-EBG for no sample ($\epsilon_r = 1$).

($<$ 1.5 ns) in the group delay at 8.00 GHz and 11.50 GHz are observed due to improper impedance matching as shown in Figure 9(b) for no sample, without EBG, and other cases. Compared to the distortion at notch band frequency, these unwanted pulse distortions are very small. Figure 11 presents simulated and measured radiation patterns of the HMA with MS-EBG for no sample case in the E-plane and H-plane at 4.00 GHz and 7.50 GHz. HMA with MS-EBG gives omnidirectional pattern in H-plane and bidirectional pattern in E-plane, and there is very litlle effect of the presence of the MS-EBG near

feed line.

The two layer HMAs with and without MS-EBG with grooved substrate are fabricated by using PCB technology using an FR4 substrate with $\epsilon_r = 4.4$, $h_1 = h_2 = 0.8\,\mathrm{mm}$, and $\tan(\delta) = 0.02$. A $50\,\Omega$ SMA connector is connected at the end of the microstrip feed line. The measured VSWRs of the HMA with and without MS-EBG for different liquids present in the grooved substrate are demonstrated in Figure 7. As shown in Figure 7, different band notches are observed for different liquids in the grooved substrate of the MS-EBG structure. For no sample, kerosene, mineral oil, and without grooved substrate band notch center frequencies are observed at $5.32\,\mathrm{GHz}$, $5.14\,\mathrm{GHz}$, $5.04\,\mathrm{GHz}$, and $4.82\,\mathrm{GHz}$, respectively. Simulated and measured results prove that using single cell of MS-EBG structure at feed line and changing liquids in the grooved substrate, the variation in notch band frequency is obtained. The comparison of the proposed technique using MS-EBG and other reported methods to get reconfigure band notch in printed monopole antenna is presented in Table 3.

4. CONCLUSION

In this paper, a multilayer step via EBG with variable band notch in printed monopole UWB antenna has been designed, analyzed, and demonstrated. The reconfigurable characteristics of the MS-EBG are achieved by creating grooves between inner square patch and outer ring and the space between EBG cells and filling them up with liquids of different ϵ_r values like kerosene, mineral oil, etc. The change in effective ϵ_r changes the capacitance values, and the band gap center frequency of MS-EBG changes. Simulated and experimental results prove the sensor characteristics of the proposed multilayer EBG. The application of the MS-EBG to get reconfigurable band notch in HMA by placing single unit cell near feed line is also demonstrated. The different liquids are deposited in the grooved substrate of the EBG cell placed near feed line to get different band notches. The design methodology has been validated through simulated and experimental results which prove that the required band notch is obtained by changing the liquid in a grooved substrate.

REFERENCES

1. Liang, J., C. C. Chiau, X. Chen, and C. G. Parini, "Study of a printed circular disc monopole antenna for UWB systems," *IEEE Trans. Antennas Propag.*, Vol. 53, No. 11, 3500–3504, 2005.

2. Srifi, M. N., S. K. Podilchak, M. Essaaidi, and Y. M. M. Antar, "Compact disc monopole antennas for current and future Ultrawideband (UWB) applications," *IEEE Trans. Antennas Propag.*, Vol. 59, No. 12, 4470–4480, 2011.

3. Cho, Y. J., K. H. Kim, D. H. Choi, S. S. Lee, and S.-O. Park, "A miniature UWB planar monopole antenna with 5-GHz band-rejection filter and the time-domain characteristics," *IEEE Trans. Antennas Propag.*, Vol. 54, No. 5, 1453–1460, 2006.

4. Dong, Y. D., W. Hong, Z. Q. Kuai, and J. X. Chen, "Analysis of planar ultrawideband antennas with on-ground slot band-notched structures," *IEEE Trans. Antennas Propag.*, Vol. 57, No. 07, 1886–1893, 2009.

5. Chu, Q. X. and Y. Y. Yang, "A compact ultrawideband antenna with 3.4/5.5 GHz dual band-notched characteristics," *IEEE Trans. Antennas Propag.*, Vol. 56, No. 12, 3637–3644, 2008.

6. Ryu, K. S. and A. A. Kishk, "UWB antenna with single or dual band-notches for lower WLAN band and upper WLAN band," *IEEE Trans. Antennas Propag.*, Vol. 57, No. 12, 3942–3950, 2009.

7. Abbosh, A. M. and M. E. Bialkowski, "Design of UWB planar band-notched antenna using parasitic elements," *IEEE Trans. Antennas Propag.*, Vol. 57, No. 03, 796–799, 2009.

8. Kim, K. H. and S. O. Park, "Analysis of the small band-rejected antenna with the parasitic strip for UWB," *IEEE Trans. Antennas Propag.*, Vol. 54, No. 06, 1688–1692, 2006.

9. Lui, W. J., C. H. Cheng, Y. Cheng, and H. Zhu, "Frequency notched ultra-wideband microstrip slot antenna with fractal tuning stub," *Electron. Lett.*, Vol. 41, No. 6, 294–296, 2005.

10. Gao, Y., B. L. Ooi, and A. P. Popov, "Band-notched ultra-wideband ring-monopole antenna," *Microw. Opt. Technol. Lett.*, Vol. 48, No. 01, 125–126, 2006.

11. Thomas, K. G. and M. Sreenivasan, "A simple ultrawideband planar rectangular printed antenna with band dispensation," *IEEE Trans. Antennas Propag.*, Vol. 58, No. 01, 27–34, 2010.

12. Qu, S. W., J. L. Li, and Q. Xue, "A band-notched ultrawideband printed monopole antenna," *IEEE Antennas Wireless Propag. Lett.*, Vol. 5, 495–498, 2006.

13. Peng, L. and C. L. Ruan, "UWB band-notched monopole antenna design using electromagnetic-bandgap structures," *IEEE Trans. Microw. Theory Tech.*, Vol. 59, No. 4, 1074–1081, 2011.

14. Bhavarthe, P. P., S. S. Rathod, and K. T. V. Reddy, "A compact dual band gap electromagnetic band gap structure," *IEEE Trans. Antennas Propag.*, Vol. 67, No. 01, 596–600, 2019.

15. Bhavarthe, P. P., S. S. Rathod, and K. T. V. Reddy, "A compact two via hammer spanner-type polarization-dependent electromagnetic-bandgap structure," *IEEE Microw. Wireless Compon. Lett.*, Vol. 28, No. 04, 284–286, 2018.

16. Zhang, L., S. Huang, Z. Huang, C. Liu, C. Wang, Z. Wan, X. Yu, and X. Wu, "Miniaturized notched ultra-wideband antenna based on EBG electromagnetic bandgap structure," *Progress In Electromagnetics Research Letters*, Vol. 91, 99–107, 2020.

17. Tang, M. C., H. Wang, T. Deng, and R. W. Ziolkowski, "Compact planar ultrawideband antennas with continuously tunable, independent band-notched filters," *IEEE Trans. Antennas Propag.*, Vol. 64, No. 8, 3292–3301, 2016.

18. Horestani, A. K., Z. Shaterian, J. Naqui, F. Martín, and C. Fumeaux, "Reconfigurable and tunable S-shaped split-ring resonators and application in band-notched UWB antennas," *IEEE Trans. Antennas Propag.*, Vol. 64, No. 09, 3766–3776, 2016.

19. Han, L., J. Chen, and W. Zhang, "Compact UWB monopole antenna with reconfigurable band-notch characteristics," *International J. of Microwave and Wireless Tech.*, Vol. 12, No. 03, 252–258, 2020.

20. Shome, P. P., T. Khan, and R. H. Laskar, "CSRR-loaded UWB monopole antenna with electronically tunable triple band-notch characteristics for cognitive radio applications," *Microw. Opt. Technol. Lett.*, Vol. 62, No. 09, 2919–2929, 2020.

21. Quddious, A., M. A. B. Abbasi, M. A. Antoniades, P. Vryonides, V. Fusco, and S. Nikolaou, "Dynamically reconfigurable UWB antenna using an FET switch powered by wireless RF harvested energy," *IEEE Trans. Antennas Propag.*, Vol. 68, No. 08, 5872–5881, 2020.

22. Nikolaou, S., N. D. Kingsley, G. E. Ponchak, J. Papapolymerou, and M. M. Tentzeris, "UWB elliptical monopoles with a reconfigurable band notch using MEMS switches actuated without bias lines," *IEEE Trans. Antennas Propag.*, Vol. 57, No. 08, 2242–2251, 2009.

23. Anagnostou, D. E., M. T. Chryssomallis, B. D. Braaten, J. L. Ebel, and N. Sepúlveda, "Reconfigurable UWB antenna with RF-MEMS for on-demand WLAN rejection," *IEEE Trans. Antennas Propag.*, Vol. 62, No. 02, 602–608, 2014.

24. Zheng, S. H., X. Liu, and M. M. Tentzeris, "Optically controlled reconfigurable band-notched UWB antenna for cognitive radio systems," *Electron. Lett.*, Vol. 50, No. 21, 1502–1504, 2014.

25. Zhao, D., L. Lan, Y. Han, F. Liang, Q. Zhang, and B.-Z. Wang, "Optically controlled reconfigurable band-notched UWB antenna for cognitive radio applications," *IEEE Photon. Technol. Lett.*, Vol. 26, No. 21, 2173–2176, 2014.

26. Saha, C., L. A. Shaik, R. Muntha, Y. M. M. Antar, and J. Y. Siddiqui, "A dual reconfigurable printed antenna: Design concept and experimental realization," *IEEE Antennas & Propag. Mag.*, Vol. 06, No. 03, 66–74, 2018.

27. Haupt, R. L. and M. Lanagan, "Reconfigurable antennas," *IEEE Antennas & Propag. Mag.*, Vol. 55, No. 01, 49–61, 2013.

28. Sievenpiper, D., L. Zhang, R. F. J. Broas, N. G. Alexopolous, and E. Yablonovitch, "High impedance electromagnetic surfaces with a forbidden frequency band," *IEEE Trans. Microw. Theory Tech.*, Vol. 47, No. 11, 2059–2074, 1999.

29. Ghosh, S., T.-N. Tran, and T. Le-Ngoc, "Dual-layer EBG-based miniaturized multi-element antenna for MIMO systems," *IEEE Trans. Antennas Propag.*, Vol. 62, No. 8, 3985–3997, 2014.

30. Yang, F. and Y. Rahmat-Samii, "Microstrip antennas integrated with electromagnetic Band-Gap (EBG) structures: A low mutual coupling design for array applications," *IEEE Trans. Antennas Propag.*, Vol. 51, No. 10, 293–2946, 2003.

31. Parvathi, K. S. L., S. R. Gupta, and P. P. Bhavarthe, "A novel compact electromagnetic band gap structure to reduce the mutual coupling in multilayer MIMO antenna," *Progress In Electromagnetics Research*, Vol. 94, 167–177, 2020.

32. Jun, S. Y., B. S. Izquierdo, and E. A. Parker, "Liquid sensor/detector using an EBG structure," *IEEE Trans. Antennas Propag.*, Vol. 67, No. 5, 3366–3373, 2019.

33. Kiani, S., P. Rezaei, and M. Navaei, "Dual-sensing and dual frequency microwave SRR sensor for liquid samples permittivity detection," *Elsevier Measurement*, Vol. 160, Art. No. 107805, Aug. 2020.

34. Remski, R., "Analysis of photonic bandgap surfaces using ansoft HFSS," *Microwave J.*, Vol. 43, No. 9, 190–199, 2000.

35. Liang, L., C. H. Liang, L. Chen, and X. Chen, "A novel broadband EBG using cascaded mushroom-like structure," *Microw Opt. Technol Lett.*, Vol. 50, No. 08, 2167–2170, 2008.

36. Yang, L., M. Fan, F. Chen, J. She, and Z. Feng, "A novel compact Electromagnetic-Bandgap (EBG) structure and its application for microwave circuits," *IEEE Trans. Microw. Theory Tech.*, Vol. 53, No. 1, 183–190, 2005.

37. Bhattacharya, A., B. Roy, S. K. Chowdhury, and A. K. Bhattacharjee, "Compact slotted UWB monopole antenna with tuneable band-notch characteristics," *Microw Opt. Technol Lett.*, Vol. 59, No. 9, 2358–2365, 2017.